Modelling Results of Covered PVT Collectors regarding Low-E Coatings and F'

Manuel Lämmle, Thomas Kroyer, Stefan Fortuin and Michael Hermann

Fraunhofer Institute for Solar Energy Systems ISE, Heidenhofstr. 2, 79110 Freiburg, Germany

Abstract

Photovoltaic-thermal (PVT) collectors are hybrid collectors which make, in principle, optimal use of the solar resource by co-generating electricity and heat in a single module. The development of innovative PVT concepts is based on a deep understanding of the interplay between design and materials, performance coefficients, and finally the thermal and electrical energy yield. Amongst others, the energy yield is influenced by the low emissivity (Low-E) coating, thermal insulation, and the thermal coupling of absorber and fluid characterized by the collector efficiency factor F'. In this paper, a modelling approach is presented which describes the interplay between optical properties of Low-E coatings, overall heat losses and F'. In analyzing seven different Low-E coatings, the complex interdependence of these three factors becomes clear. A further highlight will be put on the thermal coupling of the fluid to the absorber and its influence on F'. In addition, system simulations for a combi system are carried out to analyze the annual electricity and thermal yields.

Keywords: photovoltaic-thermal collector, collector model, Low-E coating, system simulations

1. Introduction

Solar cell convert solar radiation into electricity by making use of the photovoltaic effect. Owing to the physical limitations of conventional solar cells, less than 20 % of the incoming radiation is converted into electricity while the major share is transformed into waste heat. PVT collectors make use of this waste energy by transferring heat from the solar cell to a fluid. Thus the solar cell functions as the absorber, which is thermally coupled to a heat removal construction, e.g. a metal sheet-tube fluid heater.

Currently, the market is dominated by unglazed PVT collectors, where the focus lies on the generation of electricity while heat is delivered at low temperatures. Their field of application is therefore limited to water preheating or coupling to heat pumps. Glazed PVT collectors have their focus on the generation of heat at higher temperatures, while the electrical yields are slightly lower because of an extra cover and higher operating temperatures which reduce the PV efficiency. Concentrated PVT collectors are able to deliver heat at even higher temperatures. The setup of a typical glazed liquid flat-plate water PVT collector is shown in Fig. 1.
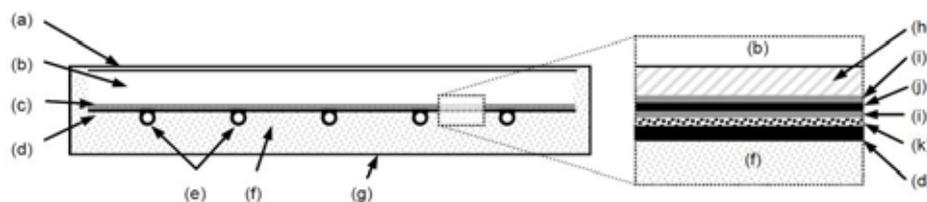

Fig. 1: Schematic setup of a glazed liquid PVT collector with (a) glass cover, (b) air layer, (c) PV module, (d) metal sheet, (e) metal tubes, (f) thermal insulation, (g) frame, (h) PV module glass, (i) EVA layer, (j) solar cell, (k) Tedlar layer + adhesive (Dupeyrat 2010).

Zondag et al. (2008) see the greatest market potential for glazed liquid PVT collectors for domestic hot

water, possibly combined with space heating. Next to commercial and certification issues, high stagnation temperatures and relatively low efficiency are the limiting factors on the technical side. For the development of innovative glazed liquid PVT collector concepts, collector models and system simulations are essential to investigate new collector design and materials, operating temperatures and energy yields. In this paper, an integral modelling approach is presented. By means of two examples – Low-E coatings and the collector efficiency factor F' – modelling results from design studies for glazed liquid PVT collectors are presented.

2. Integral Modelling Approach

The goal of the integral modelling approach is the analysis of the influence of design parameters on performance coefficients and energy yields. With this approach, new PVT collector concepts can be analyzed and optimized by varying single design parameters or the entire collector design. The approach is divided into two stages: In the first stage, characteristic performance coefficients are calculated from optical and thermal design parameters using a PVT collector model. In the second stage, these performance coefficients are used in a system simulation environment to calculate annual energy yields for typical applications. As depicted in Fig. 2, optics, thermal insulation and the thermal coupling of absorber and fluid are strongly interconnected. As most heat transfer coefficients are temperature dependent, a change of one design parameter affects most other performance coefficients. This integral modelling approach helps to understand the interplay of design parameters and develop technically and economically optimized PVT collectors.
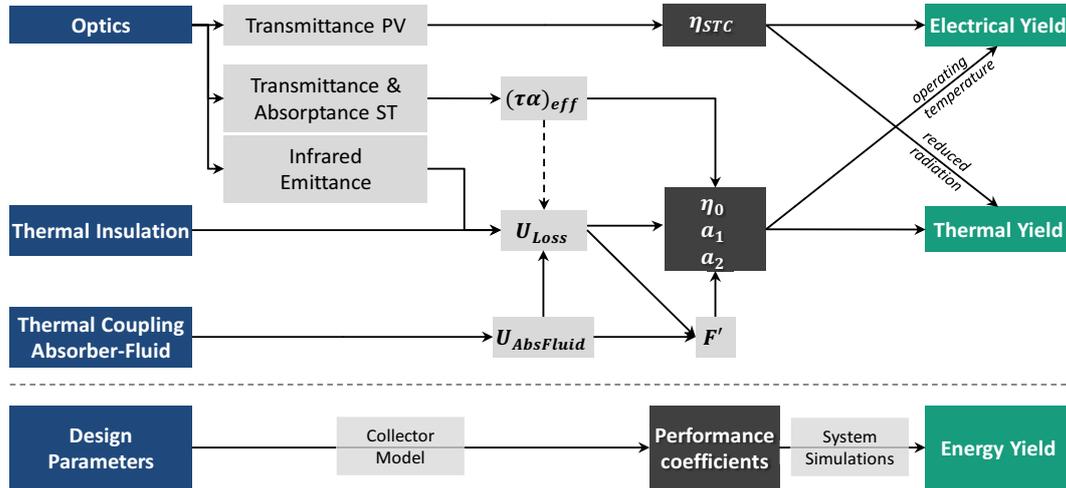

Fig. 2: Integral modelling approach covering the chain from design parameters to performance coefficients and energy yields.

The collector model is a steady-state 1D thermal resistance network which is implemented in an object-orientated simulation framework. Fig. 3 depicts the nodal model according to Helmers and Kramer (2013): The incoming radiation is first reduced by optical losses; the remaining radiation P_{abs} reaches the absorber and is then split into electricity P_{el}, useful thermal energy $\dot{Q}_{useful}$, and thermal losses $\dot{Q}_{Loss}$. The energy balance of the collector reads as follows:

$$G = P_{OpticalLosses} + P_{abs} = P_{OpticalLosses} + P_{el} + \dot{Q}_{useful} + \dot{Q}_{Loss} \qquad \text{(eq. 1)}$$

The electricity output P_{el} decreases linearly with the cell temperatures and is calculated with the extension by Florschuetz (1979), where η_{el} is the instantaneous electrical efficiency, η_{STC} the electrical efficiency under standard testing conditions, β the relative temperature coefficient of the electrical efficiency and T_{ref} the reference testing temperature:

$$P_{el} = G\eta_{el} = G\eta_{STC}(1 - \beta(T_{absorber} - T_{ref})) \qquad \text{(eq. 2)}$$

The heat transfer coefficients U_{Loss} and $U_{AbsFluid}$ are both dependent on temperature and modelled using a network of empirical and analytical thermal resistances for each heat transfer phenomenon occurring inside the collector. The detailed description of the underlying formulas lies beyond the scope of this paper and can

be found in secondary literature such as Zondag et al. (2002), Matuska (2009) and Dupeyrat (2011).
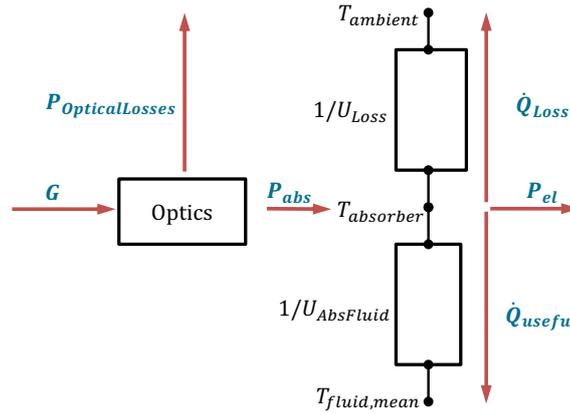

Fig. 3: Energy balance of a PVT collector for a one-dimensional collector model according to Helmers and Kramer (2013).

The collector model is run with varying fluid temperatures. Then, the characteristic performance coefficients η_0, a_1, a_2 are extracted with statistical curve fitting using the least square method to obtain an instantaneous efficiency curve according to the international standard ISO 9806:2013(E) :

$$\eta = \frac{\dot{Q}_{useful}}{G \, A_{aperture}} = \eta_0 - a_1 \frac{T_{fluid,mean} - T_{ambient}}{G} - a_2 \frac{(T_{fluid,mean} - T_{ambient})^2}{G} \qquad \text{(eq. 3)}$$

with the conversion factor η_0

$$\eta_0 = F' K_\theta (\tau\alpha)_{eff} \qquad \text{(eq. 4)}$$

where K_θ is the incidence angle modifier and $(\tau\alpha)_{eff}$ the effective transmittance-absorptance product.

System simulations are carried out in TRNSYS using the reference heating system of Task 32 defined by Heimrath and Haller (2007). The reference building consists of a two-story single family house with a specific heating load of 60 kWh/m²a and a domestic hot water demand of 175 l/day located in Würzburg, Germany. The aperture area of the PVT collector field amounts to 12 m². A stratified storage tank with a volume of 900 l is used. Regarding the PVT collector, available TRNSYS types are not sufficient as the dependence of the electrical yield on the mean absorber temperature is not well implemented in these types. Instead, the solar thermal collector Type 832 (Haller et al. 2012) is coupled to a custom PV type. Type 832 is run in CMode 2, where the absorber and the fluid nodes are coupled via the heat transfer coefficient $U_{AbsFluid}$. Performance coefficients obtained with the collector model in MPP (maximum power point) mode are employed. Regarding the electricity yield, the temperature of the absorber node is used for the calculation of the instantaneous PV efficiency η_{el} using eq. 2. In the event of stagnation, empirical formulas for the absorber temperature are applied, since an extrapolation of the efficiency curve would lead to an underestimation of the stagnation temperature. As an indicator for the thermal performance, the extended fractional energy savings $f_{sav,ext}$ quantify the percentage of saved primary energy including parasitic electricity consumption. Additionally the specific thermal and electrical yields of the PVT collector are specified, which are fed into the thermal storage and public electricity grid, respectively.

3. Design Study regarding Low-E Coatings

In order to increase the thermal performance of PVT collectors, thermal losses need to be reduced. One approach is based on spectrally selective Low-E coatings which have a high reflectance in the infrared spectrum similar to absorber coatings for solar thermal collectors but with high transmittance instead of high absorptance in the visible spectrum. The spectral selectivity can be achieved by applying a layer stack composed of a thin transparent metal (e.g. silver) combined with transparent oxides or by using transparent conductive metal oxides (e.g. indium tin oxide or doped zinc oxide). The desired environmental stability can be achieved by the suitable choice of layer materials, layer stack, and production process (Giovanetti et al. 2014).

For the scope of this design study, four commercial Low-E coatings, one in-house development of Fraunhofer ISE, and one PV module glass without Low-E are selected. They represent the whole range from very low emittance ($\varepsilon = 0.08$ at 100 °C) to high emittance ($\varepsilon = 1$). For all six configurations, reflectance and emittance are measured in-house with a spectral reflectometer using an Ulbricht sphere. The measured spectra are weighted with the AM 1.5 spectrum and spectral response for PV efficiency, AM 1.5 for thermal efficiency, and the black body radiation at 100 °C for emittance. Furthermore, multiple reflections, suppressed backside reflections, and the absorptance of PV cells are taken into consideration. Thus, the electrical PV efficiency η_{STC} and the effective transmittance-absorptance product $(\tau\alpha)_{eff}$ are derived for each configuration.

Inside the PVT collector, the Low-E coating is located at position 3 on top of the PV module glass. With the Low-E coating at position 2, i.e. inner side of the front cover, radiative losses are identical. However, owing to the finite absorptance of Low-E coatings in the range of $\alpha_{AM1.5} = 0.06 - 0.12$, this absorbed energy can thus be transferred to the fluid resulting in an enhanced $(\tau\alpha)_{eff}$. Regarding the front glass cover, a 3.2 mm low-iron glass with double-sided anti-reflective coating with a transmittance of $\tau_{AM1.5}=0.96$ is used. The collector is well insulated with a moderate coupling of absorber to the fluid with $U_{AbsFluid} = 60 \frac{W}{m^2 K}$ (compare section 4 for an interpretation of this value).

While optimizing thermal performance, Low-E coatings go at the expense of electrical performance because of higher reflectance and absorptance: The employed PV module has a certified efficiency of $\eta_{STC} = 15.9\,\%$ under standard testing conditions (STC). Through the presence of the front glass, the module efficiency is reduced by $3\%_{rel}$; through the application of Low-E coatings, the module efficiency is further reduced by $5 - 13\,\%_{rel}$ resulting in an electrical efficiency of the PVT collector of $\eta_{STC} = 13.4 - 14.7\,\%$. The efficiency curves for five PVT collectors with Low-E coatings ($\varepsilon=0.08 - \varepsilon=0.4$) and one with standard PV module glass ($\varepsilon=1$) are shown in Fig. 4.
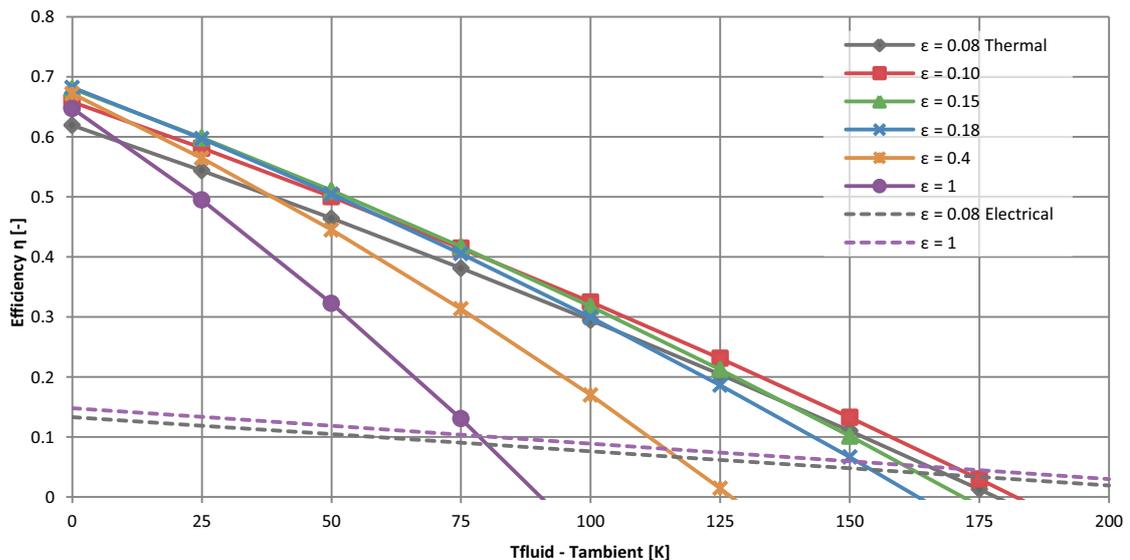

Fig. 4: Thermal and electrical efficiency curves for six PVT collectors with various Low-E coatings in MPP mode at G=1000 W/m² and u_wind=3 m/s relative to aperture area.

The inclination of the efficiency curves is determined by the overall heat loss coefficient U_{Loss}. For the PVT collector without Low-E coating, the overall heat losses comprise radiation between the glass panes (63 %), convection in the air layer (25 %), back (10 %) and edge losses (3 %) at $T_{fluid} - T_{ambient} = 50\,K$. The radiative losses are reduced significantly by Low-E coatings resulting in a lower inclination of the efficiency curve (compare Fig. 7). Regarding the conversion factor η_0, an interesting effect is observed: With lower emittance, $(\tau\alpha)_{eff}$ decreases due to optical losses. At the same time, U_{Loss} decreases owing to less radiative losses. As a consequence, F' increases (compare eq. 5). Therefore, there exists an optimum with regards to the conversion factor η_0, which is achieved for the given PVT collector configurations by Low-E coating $\varepsilon = 0.18$. The influence of the obtained thermal and electrical performance coefficients on the annual energy yield is shown in Fig. 5.
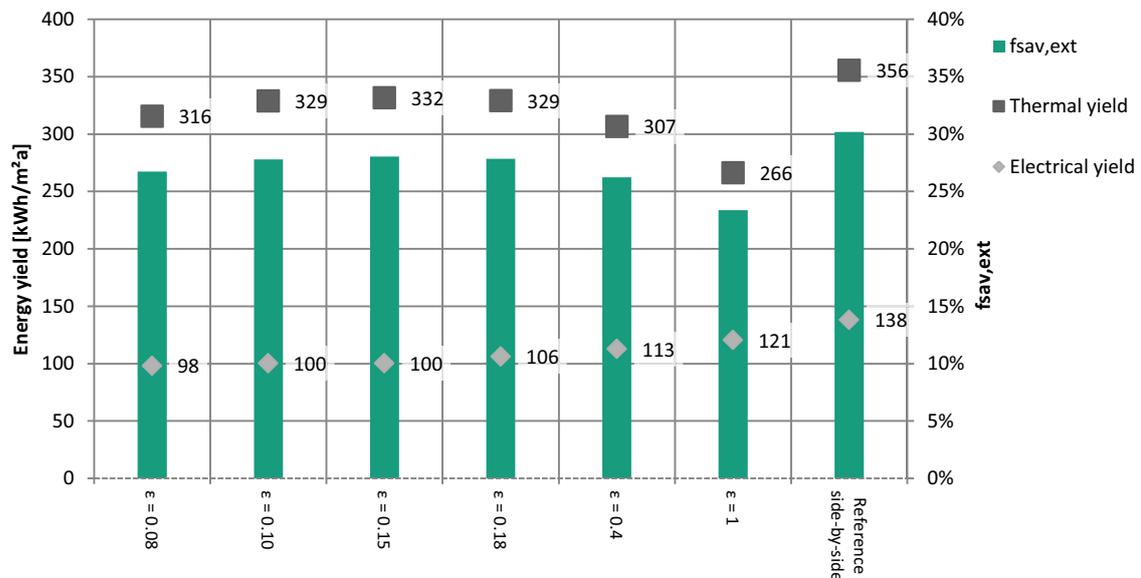
Fig. 5: Thermal and electrical yield for six modeled PVT collectors and a reference case with a solar thermal collector and PV module side-by-side. Specific yields are expressed relative to an aperture area of 12 m².

The maximum thermal yield is achieved by Low-E coating $\varepsilon = 0.15$ with a specific thermal yield of 332 kWh/m²a and thus only 7 % less than a standard solar thermal flat plate collector with a spectrally selective absorber coating. The reduction of available radiation due to electricity production is for one part compensated by a double AR coated front cover instead of a standard front cover. For the other part, the extracted electricity serves as a heat sink resulting in lower absorber temperatures and therefore lower thermal losses compared to the operation in the open circuit mode. As expected, the maximum electrical yield is achieved by the PVT collector without Low-E coating with a specific electrical yield of 121 kWh/m²a and thus only 12.8 % less than a standard PV module. The reduced electrical output is caused in equal parts by elevated operating temperatures (6.4 %) and deteriorated optics (6.4 %).

Depending on the weighting of thermal to electrical yield, one can select the optimal Low-E coating. Up to a weight of electricity to heat of 3:1, Low-E coating $\varepsilon = 0.18$ is favored; for a weight of 4:1 Low-E coating $\varepsilon = 0.4$. For higher weights, no Low-E coating ($\varepsilon = 1$) delivers the optimal configuration. For comparison purposes, the new European building directive according to DIN EN 15603:2013-05 provides a weight of 2.31:1, which favors Low-E coating $\varepsilon = 0.18$. This analysis is highly sensitive towards the system the PVT collector is integrated into. Depending on the demand and climate specifications regarding fluid temperatures and seasonal profile, other types of PVT collector might be favorable than the optimal collector for a combi system in Western Europe. The context of system, application and heat demand is therefore centrally important for the decision in favor of Low-E coatings, or even glazed, unglazed, or concentrating PVT collectors.

4. Design Study regarding F'

The collector efficiency factor F' is no design parameter such as Low-E coatings or tube spacing, but a measure obtained from performance measurements at the operating point $T_{fluid,mean} - T_{ambient} = 0$. There, the mean fluid temperature is kept at the ambient temperature while the absorber temperature lies higher, depending on the thermal coupling of absorber to the fluid. This is why even at the so called "optical efficiency" or "zero-loss efficiency" η_0 significant thermal losses to the ambient occur[1]. Duffie and Beckman (2013) define F' as the ratio of the actual useful energy gain to the useful gain that would result if the collector absorbing surface had been at the local fluid temperature. For most geometries, this definition can be interpreted as the ratio of U_0 to U_{Loss}, where U_0 is the heat loss coefficient from fluid to ambient. As

---

[1] In fact, even when the absorber temperature equals the ambient temperature, radiative heat exchange from the absorber to the colder sky temperature takes place. This phenomenon is technically used in night cooling with unglazed collectors.

illustrated in Fig. 3, $1/U_0$ represents a series connection of the two thermal resistances $\frac{1}{U_{AbsFluid}}$ and $\frac{1}{U_{Loss}}$ (compare eq. 5) leading to the formulation of F' as in eq. 5:

$$F' = \frac{U_0}{U_{Loss}} = \frac{\left[\frac{1}{U_{AbsFluid}}+\frac{1}{U_{Loss}}\right]^{-1}}{U_{Loss}} = \frac{1}{1+\frac{U_{Loss}}{U_{AbsFluid}}}$$

(eq. 5)

As demonstrated above, the definition of F' is rather unintuitive, especially with regard to the non-linearity and temperature dependence of U_{Loss}. Therefore, the heat transfer coefficient $U_{AbsFluid}$ is used instead to quantify the thermal coupling of absorber to fluid. $U_{AbsFluid}$ is a variable solely influenced by design parameters such as tube spacing, tube diameter, thickness of absorber plate, and fluid flow and is independent from U_{Loss}.

For sheet-and-tube absorbers, analytical approaches for the calculation of $U_{AbsFluid}$ and F' are described extensively in Duffie and Beckman (2013). In PVT collectors, the absorbing structure is made up by solar cells, which are coupled to the fluid by several layers of different materials, thicknesses, and thermal conductivities resulting in two-dimensional heat fluxes from absorber to fluid. Therefore the heat transfer coefficient $U_{AbsFluid}$ is assessed with a 2D finite element approach (compare Koch et. al (2012) and Góngora-Gallardo et al. (2013)). Using realistic boundary conditions, $U_{AbsFluid}$ can be evaluated with eq. 6, where $\dot{q}_{useful}$ is the specific heat flux from absorber to the fluid.

$$U_{AbsFluid} = \dot{q}_{useful}(T_{absorber,mean} - T_{fluid,mean})$$

(eq. 6)

The 2D model and resulting temperature distribution is shown in Fig. 6 for a tube distance of 110 mm, tube diameter of 10 mm and $\alpha_{fluid} = 300 \, W/m^2K$ leading to $U_{AbsFluid} = 60 \, W/m^2K$.
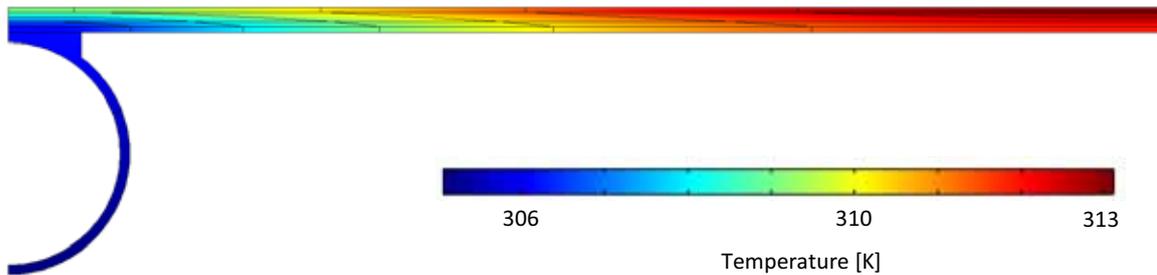

306   310   313

Temperature [K]

Fig. 6: 2D finite element model for an absorber segment with temperature distribution and isotherms at $\Delta T = 0K$.

In this design study, the thermal coupling between absorber and fluid is varied between $U_{AbsFluid} = 20 \, W/m^2K$ for poor thermal coupling and $U_{AbsFluid} = 120 \, W/m^2K$ for good thermal coupling. A more comprehensive interpretation of these values delivers the notion that the poor case represents a tube spacing of 170 mm and the good case a tube spacing of 55 mm. Using absorbers, where the fluid contacts the entire surface, such as roll bond absorbers or rectangular ducts, even higher heat transfer coefficients can be achieved. The six input values of $U_{AbsFluid}$ are used as givens in the collector model. There, a sophisticated thermal resistance network is solved iteratively until the energy balance for the temperature dependent thermal resistances converges. The overall heat loss coefficient U_{Loss} strongly depends on the absorber temperature as shown in Fig. 7. The heat loss rate at $T_{absorber} = T_{ambient}$ results from the temperature of the front cover being lower than ambient temperature, owing to radiative losses to the cold sky. Therefore, U_{Loss} goes to infinity at that point. A minimum is reached for U_{Loss} at $\Delta T = 18 \, K$. Beyond that point, U_{Loss} grows, owing to the non-linearity of radiation and temperature dependent fluid and solid properties.
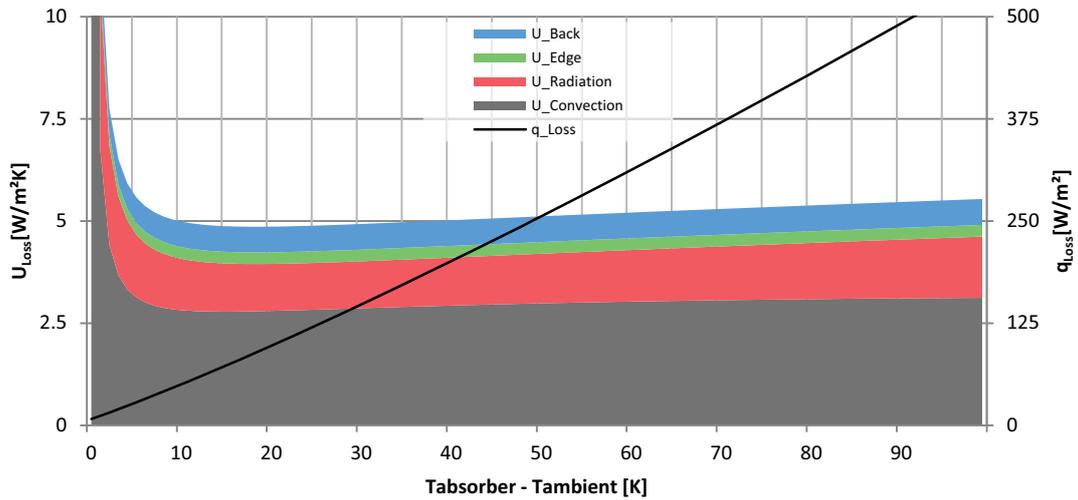
Fig. 7: Overall heat loss coefficient U_{Loss} as function of the temperature difference between absorber and ambient, for a PVT collector with Low-E coating ε=0.18 at G=1000 W/m² and u$_{wind}$=3 m/s.

The heat transfer coefficient between absorber and fluid $U_{AbsFluid}$ strongly influences the absorber temperature, which on the other hand determines U_{Loss}. At ΔT = 0 K, the difference between absorber and fluid temperature amounts to 32 K for the poor case and merely 2 K for the good case. Taking into consideration that elevated absorber temperatures reduce the electrical efficiency, one realizes the importance of a good thermal contact. The resulting thermal and electrical efficiency curves for the PVT collector with Low-E coating $\varepsilon = 0.18$ are plotted in Fig. 8. With given $(\tau\alpha)_{eff}$ and K_θ, the corresponding F' is derived from eq. 5.

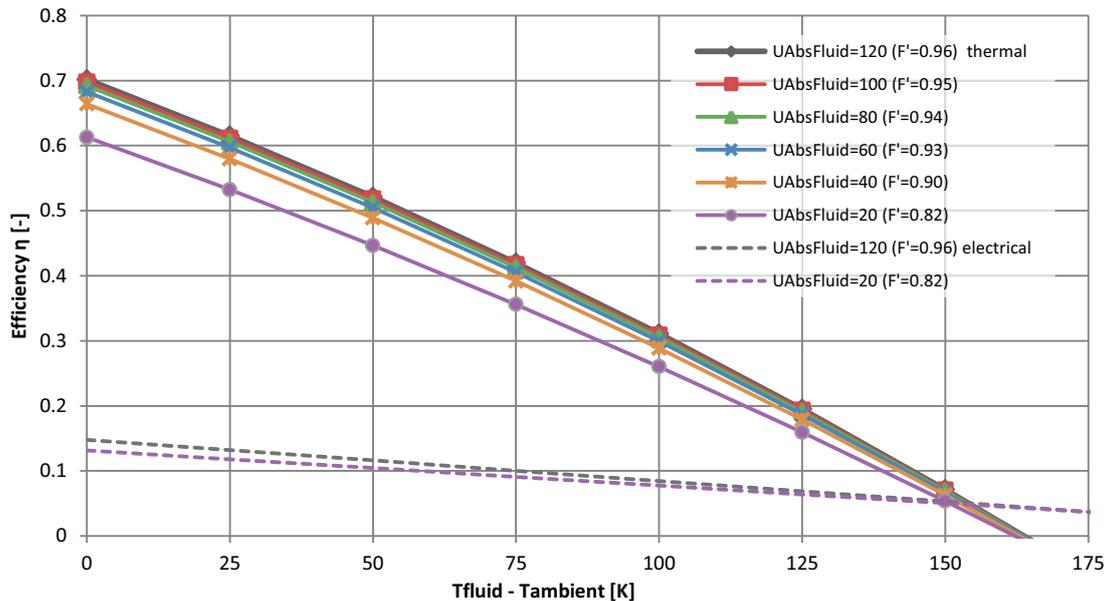**Fig. 8: Thermal and electrical efficiency curves for six PVT collectors with ε=0.18 and varying thermal coupling in MPP mode at G=1000 W/m² and u$_{wind}$=3 m/s relative to aperture area.**

The resulting collector efficiency factor F' varies between 0.82 ($U_{AbsFluid} = 20\ W/m^2K$) and 0.96 ($U_{AbsFluid} = 120\ W/m^2K$). Stagnation temperatures are independent from thermal coupling, which is logical considering that heat flux and thus temperature difference from absorber to fluid equal zero at this point. For $U_{AbsFluid} > 60$ W/m²K, no substantial improvements regarding efficiency and F' can be observed.

For PVT collectors with higher thermal losses, a good thermal coupling becomes more and more important. Because of the dependence of F' from U_{Loss}, F' decreases considerably for higher thermal losses as shown in Tab. 1 at the example of six different PVT collector configurations. Without the use of Low-E, F' drops from

0.96 to 0.92 for $U_{AbsFluid} = 120\ W/m^2K$. In the case of a poor thermal coupling ($U_{AbsFluid} = 20\ W/m^2K$), F' even decreases from 0.82 to 0.72. Unglazed PVT collectors have significantly higher convective losses because of the absence of a front cover. For these types of collectors, U_{Loss} typically amounts to $20 - 30$ W/m²K and thus 4 - 5 times higher than for glazed PVT collectors with Low-E: The same absorber design for good thermal coupling ($U_{AbsFluid} = 120\ W/m^2K$) results in a significant reduction of F' to 0.78. In the case of poor thermal coupling ($U_{AbsFluid} = 20\ W/m^2K$), F' drops to 0.49. This illustrates why not only the thermal coupling but rather the ratio of U_{Loss} to $U_{AbsFluid}$ is the crucial factor for a high collector efficiency factor F'.

Tab. 1: U$_{Loss}$ and resulting *F'* for different PVT collector configurations at the operating conditions $\Delta T = 0K$ (T$_{fluid}$=T$_{ambient}$=25 °C), G=1000 W/m², and u$_{wind}$=3 m/s.

		Glazed, Low-E		Glazed, No Low-E		Unglazed, No Low-E	
Emittance ε	[-]	0.18		1		1	
$U_{AbsFluid}$	[W/m²K]	20	120	20	120	20	120
$T_{Absorber,mean}$	[°C]	48	31	51	31	44	30
U_{Loss}	[W/m²K]	4.6	5.8	7.9	10.1	20.4	29.6
F'	[-]	0.82	0.96	0.72	0.92	0.49	0.80

The results of system simulations are shown in Fig. 9. Improving F' from 0.82 to 0.96 results in an increase of 3.1 % in thermal yield or likewise an increase of the extended fractional energy savings from $f_{sav,ext} = 27.2\ \%$ to $f_{sav,ext} = 28.1\ \%$. The electrical yield increases by 2.3 % at the same time. With $F' > 0.9$ or $U_{AbsFluid} > 40\ W/m^2K$ respectively, good results for both thermal and electrical yields can be realized for PVT collectors with Low-E coatings. An improvement of the thermal contact beyond this point leads to a further increase of only 1.3 % for thermal yield or 1.0 % for electrical yield, respectively.
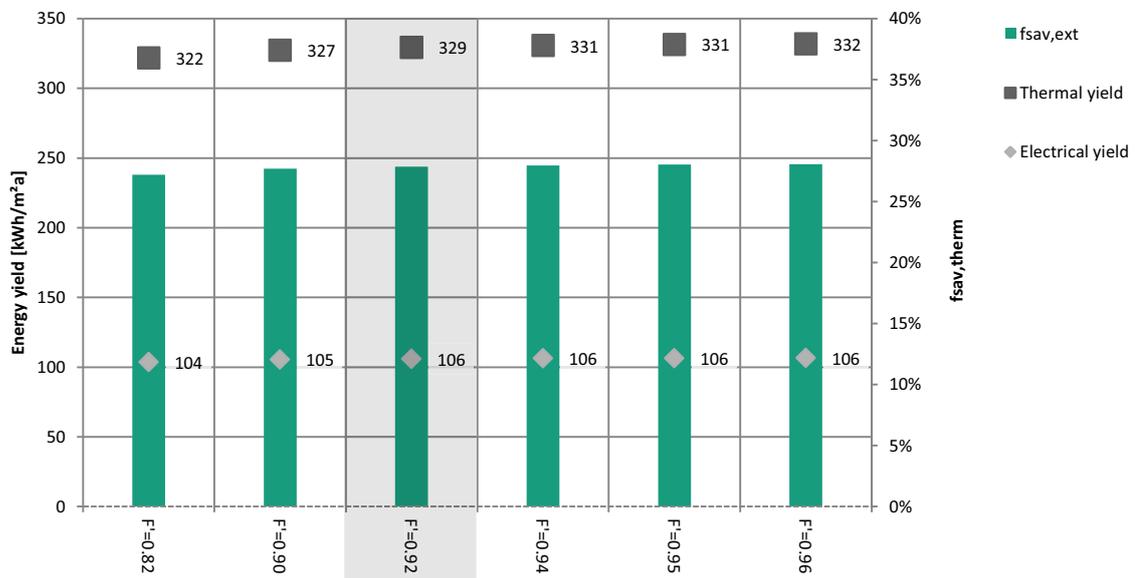

Fig. 9: Thermal and electrical yield for six modeled PVT collectors systems with reference scenario F'=0.92. Specific yields are expressed relative to an aperture area of 12 m².

To conclude, a good thermal contact between absorber and fluid is important for both electrical and thermal efficiency. Electrical and thermal yield benefit in the same way from a good thermal coupling, which is why the optimization of F' is a mere economical question. In the end, the decision towards a good thermal contact needs to be made on basis of higher yield vs. high material usage, production cost and pressure drop of the collector.

5. Conclusion and Outlook

The presented integral modelling approach is a suitable tool for the development and optimization of new PVT collector designs. For these collectors, electrical and thermal performances are closely interconnected: both optical and thermal design parameters influence the performance parameters on the electrical and thermal side. With the collector model, these interdependencies are modelled by solving energy balances in a thermal resistance network. During operation, the electrical and thermal outputs are also closely interconnected: PV reduces the available solar radiation while operation temperatures inside the PVT collector determine the instant electrical efficiency. With system simulations these relationships are modelled for a domestic combi system. Under any circumstances, the results of the design optimization strongly depend on the underlying system. Thermal and electrical supply of the PVT collector need to be matched to the thermal and electrical demand of the PVT system for highest yields. The presented modelling approach allows such a system orientated approach of component development.

By means of the examples of Low-E coatings and F' a design study for glazed PVT collectors is carried out. Low-E coatings enhance the thermal performance by reducing radiative losses. At the same time, transmittance of solar radiation is reduced for the PV module. The choice for a Low-E coating is therefore a trade-off between electrical and thermal output. In contrast, the thermal coupling of absorber to fluid is a win-win for both thermal and electrical performance. As the collector efficiency factor F' is strongly dependent on thermal losses, the heat transfer coefficient $U_{AbsFluid}$ is used as the critical design parameter, instead.

Acknowledgement

References

Duffie, J.A., Beckman, W.A., 2013. Solar engineering of thermal processes. John Wiley & Sons.

Dupeyrat, P., Ménézo, C., Wirth, H., Hofmann, P., Kwiatkowski, G., Rommel, M., Stryi-Hipp, G., 2010 - Design of a flat-plate Photovoltaic-Thermal (PV-T) hybrid collector: modelling and experimental investigations. In Proceedings, EuroSun 2010,28.9-1.10.2010, Graz, Austria.

Dupeyrat, P., 2011. Experimental development and simulation investigation of a photovoltaic-thermal hybrid solar collector. Lyon, France, INSA Lyon. Ph.D.

Florschuetz, L.W., 1979. Extension of the Hottel-Whillier model to the analysis of combined photovoltaic/thermal flat plate collectors, Solar Energy, Volume 22, Issue 4, 1979, Pages 361-366, ISSN 0038-092X.

Giovannetti, F., Föste, S., Ehrmann, N., Rockendorf, G., 2014. High transmittance, low emissivity glass covers for flat plate collectors: Applications and performance. Solar Energy, Solar heating and cooling 104, 52–59. doi:10.1016/j.solener.2013.10.006

Góngora-Gallardo, G., Castro-Gil, M., Colmenar-Santos, A., Tawfik, M., 2013. Efficiency factors of solar collectors of parallel plates for water. Solar Energy 94, 335–343. doi:10.1016/j.solener.2013.05.014

Haller, M., Perers, B., Bale, C., Paavilainen, J., Dalibard, A., Fischer, S., Bertram, E., 2012. TRNSYS Type 832 v5. 00 „Dynamic Collector Model by Bengt Perers ", SPF.

Heimrath, R., Haller, M., 2007. The reference heating system, the template solar system of Task 32. A report of IEA Solar Heating and Cooling programme–Task 32.

Helmers, H. and Kramer, K., 2013. Multi-linear performance model for hybrid (C)PVT solar collectors. Solar Energy 92: 313-322.

International Stadard ISO 9806:2013(E) Solar energy — solar thermal collectors — test methods, edition 2013-11.

Koch, L., Hermann, M., Bauch, M., 2012 - Investigation of a new integrated solar thermal absorbers by means of a 2-D model. In Proceedings, EuroSun 2012, 18.9-20.9.2012, Rijeka, Croatia.

Matuska, T., Zmrhal, V., 2009. KOLEKTOR 2.2 – reference handbook. 3rd draft. ed. Prague: Czech Technical University.

Zondag, H.A., de Vries, D.W., van Helden, W.G.J., van Zolingen, R.J.C., van Steenhoven, A.A., 2002. The thermal and electrical yield of a PV-thermal collector. Solar Energy 72, 113–128. doi:10.1016/S0038-092X(01)00094-9